HHS Public Access

Author manuscript

J Neurosci Methods. Author manuscript; available in PMC 2018 October 30.

Published in final edited form as:

J Neurosci Methods. 2018 January 01; 293: 144–150. doi:10.1016/j.jneumeth.2017.09.014.

Surgical techniques influence local environment of injured spinal cord and cause various grafted cell survival and integration

Shaoping Hou[*], **Tatiana M. Saltos**, **Idiata W. Iredia**, and **Veronica J. Tom**

Spinal Cord Research Center, Department of Neurobiology & Anatomy, Drexel University College of Medicine, Philadelphia, PA, 19129, United States

Abstract

Background: Cellular transplantation to repair a complete spinal cord injury (SCI) is tremendously challenging due to the adverse local milieu for graft survival and growth. Results from cell transplantation studies yield great variability, which may possibly be due to the surgical techniques employed to induce an SCI. In order to delineate the influence of surgery on such inconsistency, we compared lesion morphology and graft survival as well as integration from different lesion methodologies of SCI.

New method: Surgical techniques, including a traditional approach cut + microaspiration, and two new approaches, cut alone as well as crush, were employed to produce a complete SCI, respectively. Approximately half of the rats in each group received injury only, whereas the other half received grafts of fetal brainstem cells into the lesion gap.

Results: Eight weeks after injury with or without graft, histological analysis showed that the cut + microaspiration surgery resulted in larger lesion cavities and severe fibrotic scars surrounding the cavity, and cellular transplants rarely formed a tissue bridge to penetrate the barrier. In contrast, the majority of cases treated with cut alone or crush exhibited smaller cavities and less scarring; the grafts expanded and blended extensively with the host tissue, which often built continuous tissue bridging the rostral and caudal cords.

Comparison with existing methods: Scarring and cavitation were significantly reduced when microaspiration was avoided in SCI surgery, facilitating graft/host tissue fusion for signal transmission.

Conclusion: The result suggests that microaspiration frequently causes severe scars and cavities, thus impeding graft survival and integration.

1. Introduction

Cell transplantation is a promising approach to improve functional recovery following spinal cord injury (SCI). The concept of transplanting early stage neurons is attributed to their capacity for differentiation and axonal growth under neuron-intrinsic mechanisms in the host (Reier, 2004; Gaillard et al., 2007). This holds the potential to reconstitute supraspinal

[*]Corresponding author: sh698@drexel.edu (S. Hou).

control of denervated caudal spinal neurons and relay signals across the lesion gap. To date, this therapeutic approach has achieved considerable positive feats by implanting fetal neurons or neural restricted precursors into a small lesion created by a contusion or incomplete transection of the rat spinal cord, whereby grafted cells expand and fill the cavity (Jakeman and Reier, 1991; Lepore and Fischer, 2005). However, unanticipated complications occurred when the cell transplantation was applied to a completely-transected spinal cord lesion (Lu et al., 2012; Sharp et al., 2014).

A SCI model with complete transection is considered the most rigorous to study axonal regeneration, as it eliminates false evaluation resulting from spared axons and their sprouting (Blesch and Tuszynski, 2003). Recently, Lu et al. transplanted embryonic spinal cord-derived neural stem cells (NSCs)/progenitors into a completely transected rat thoracic spinal cord. They reported remarkable graft-host integration, axonal growth, and locomotor functional recovery (Lu et al., 2012). Yet, a follow-up replication study did not fully duplicate these outcomes even though the same researcher conducted the surgical procedure (Sharp et al., 2014). In addition, the replication revealed severe non-neuronal partitions and large cavities at lesion/graft site in most cases. Accordingly, this caused a controversy in the original study. Though a following response from the researchers discussed the possible reasons for this discrepancy (Tuszynski et al., 2014), the real source of variability has not been ascertained. As the first step to produce an injury model, surgical techniques are critical to establish a harsh environment for cell grafting. Based on our observation and experience, we posit that variations in SCI surgical techniques affect local conditions of injury, which in turn, determine the success of subsequent cell transplantation.

To test this hypothesis, in the present study, three different surgical techniques were used to produce a complete SCI, including1) cut + microaspiration, 2) cut only, and 3) crush. Unlike previous two-week delayed transplantation, we have here grafted mechanically-dissociated fetal brainstem cells into the lesion gap immediately after injury. Donor tissues were treated and implanted as small chunks instead of single cell solutions in order to maximally preserve the embryonic extracellular matrixes (ECM). Therefore, this study was not aimed to verify reproducibility, but rather to discover the reason behind the enormous variability in cell transplantation for SCI. The findings may help indicate a more suitable injury model to optimize cell transplantation strategies for better restoration of function following SCI.

2. Materials and methods

2.1. Animals

A total of 44 adult female Fischer 344 rats weighing 150–200 g were used. Institutional Animal Care and Use Committee and Society for Neuroscience guidelines on animal care were strictly followed to minimize the number of animals used and potential suffering. Animals were anesthetized with 2% isoflurane before spinal cord surgery and cell grafting. Animals were divided into 2 cohorts: injury alone and injury plus cell graft. Based on different surgical techniques, the cohort of injury alone included1) cut + microaspiration (n = 7), 2) cut only (n = 11), and 3) crush (n = 5); whereas the cohort of injury plus graft, which consisted of embryonic day 14 (E14) brainstem-derived neural stem cells (BS-NSCs)/ progenitors, included: 4) cut + microaspiration plus cells (n = 6), 5) cut only plus cells (n =

10), and 6) crush plus cells (n = 5). Microaspiration was only applied in dura-opened surgery, whereas it was not done in crush injury (Groups 3 and 6) because the dura was not opened. In comparison to animals with cut only (Groups 2 and 5), those receiving cut + microaspiration (Groups 1 and 4) provided adequate information about the effect of microaspiration.

2.2. Surgery of SCI

All animals underwent a T3 dorsal laminectomy. In the 1st group of rats, the dura was cut longitudinally in the midline. Then the spinal cord at T4 level was completely cut using a combination of iridectomy microscissors (Fig. 1**Aa**) and subsequently aspirated with self-made aspirators. In each rat, all three aspirators were used from large to small in diameter (Fig. 1**Ab–d**), to remove spared tissue piece by piece, which was often present in the ventral and lateral edges. The 2nd group of rats received a similar dura lesion, however only a cut to the spinal cord without aspiration was performed. After infiltrated blood and fluid were absorbed with a fine tip cotton swab, visual verification ensured the completed tran-section ventrally and laterally. In the 3rd group of rats, the dura was kept intact and the spinal cord was completely crushed at T4 level for a total of 10 s with Dumont 5/45 forceps (Fig. 1**Ae**). For those receiving injury only, the overlying musculature and skin was immediately closed after hemostasis. Animals were administered with Lactated Ringer's solution (Baxter Healthcare), cefazolin (10 mg/kg), and buprenex (0.1 mg/kg) post-operatively. Bladders were manually expressed at least twice daily until sacrifice.

2.3. Cell preparation and grafting

E14 brainstem from Fischer 344 transgenic rats expressing enhanced green fluorescent protein (EGFP) under the ubiquitin C promoter provided donor tissue for grafting (Rat Resource and Research Center, University of Missouri). At this stage, the grafts are composed of a mixture of NSCs, neuronal restricted precursors, and glial restricted precursors. GFP-expressing E14 brainstem was freshly dissected and mechanically dissociated into small chunks. Then cells were resuspended in a fibrin matrix (25 mg/ml fibrinogen, 25 U/ml thrombin) containing growth factors to support graft survival as described previously (Lu et al., 2012; Hou et al., 2013). Immediately after SCI, the dura was sutured in the model with an opened dura before cell injection in order to retain cells within the lesion. E14 cells were injected into the lesion through the dura with a 10 ul Hamilton syringe in all types of injury models. A total of 8–10 μl of cells (1.0×10^6μl) were microinjected into the lesion site per rat. Musculature and skin were immediately closed. Animals were treated as described above and survived for an additional 8 weeks.

2.4. Tissue processing and immunohistochemistry

Animals were overdosed with Euthasol and perfused transcardially with 4% paraformaldehyde. To study rostro-caudal distribution of scarring and cavitation, the spinal cord was dissected and the segments spanning 0.5 cm rostral and 2.5 cm caudal to the lesion (approximate levels T2–T10) were serially cryosectioned in the longitudinal, horizontal plane at 35 μm in six series of sections (Hou et al., 2013). A serial free-floating section with interval distance of 175 μm between adjacent ones was incubated with primary antibodies

against GFAP (mouse, 1:1000 Millipore) to label astrocytes, PDGFR-β (rabbit, 1:1000; abcam) to label blood vessel-derived fibroblasts, and GFP (Chicken, 1:1000) to label transplanted cells. Double immunolabeling for GFAP and PDGFR-β was conducted in sections with injury only whereas triple labeling for GFAP, PDGFR-β and GFP were performed for grafted samples. Sections were incubated in primary antibody solution overnight at 4 °C and then incubated in Alexa Fluor 488-, 594-, or 647-conjugated goat secondary antibodies (1:500; Invitrogen) for 3 h at room temperature. After thoroughly washing, sections were mounted on the glass slide and coverslipped with Fluoromount-G medium containing DAPI (Southern Biotech). Photographs were taken using a Leica digital camera connected to a Leica DM5500 B microscope.

2.5. Lesion completeness

The completeness of lesion in the groups of cut + microaspiration or cut only was initially verified right after injury, as two spinal cord stumps retracted and a gap emerged if complete. This was not done in the group with crush injury due to the intact dura. However, lesion completeness was further verified in a serial of spinal cord sections, which were processed with double immunostaining for GFAP and PDGFR-β in animals with injury alone, or triple immunostaining for GFAP, GFP and PDGFR-β in animals with injury plus cells. In animals receiving injury without graft, the lesion was considered incomplete if a continuous $GFAP^+$tissue spanned across PDGFR-β-labeled injury site. These rats were excluded from quantification and statistical analysis, which included 1 in the group with cut + microaspiration and 2 in the group with cut alone. In animals receiving injury and cellular graft, because GFP^+grafts could also derive astrocytes, the lesion was considered incomplete if continuous $GFAP^+$but GFP^- tissues were across PDGFR-β-labeled injury site. These rats were also excluded from quantification and statistical analysis, including 1 in the group with cut plus cells and 1 in the group with crush plus cells. In a few cases in the group with cut alone (n = 2) or crush (n = 1), unusual tissue damage was perceived in the parenchyma of cord, which was not caused directly from injury *per se* due to their location away from the lesion site. As a result, these rats were also excluded from analysis. Thus, the final numbers of animals used for quantification in each group were: 6 for cut + microaspiration, 7 for cut only, 4 for crush, 6 for cut + microaspiration plus cells, 9 for cut plus cells, and 4 for crush plus cells.

2.6. Quantification and statistics

An observer blinded to group identity analyzed lesion scar size and cavitation at 100 × magnification under a microscope (Olym pus BX51). A calibrated eyepiece with a scale (from 10 to maximum 1000 μm) was used to delineate regions and cavities. In both injury only and grafted spinal sections, the lesion site was easily identified by interrupted host $GFAP^+$ astrocytes and dense infiltration of PDGFR-β^+ fibroblasts. In each animal, a total of 3 sections in the middle area of the spinal cord were chosen for the quantification of scarring and cavitation (Fig. 1**B**). As fibrotic scars typically filled the entire lesion site in animals that received injury only, we mea sured the rostro-caudal extent of PDGFR-β-labeled scars. Due to width variation of the scar from one side to another, we measured 3 different areas, including the middle, left and right edges of the sections. The values obtained from each section were then averaged. In grafted cords, however, fibrotic scars were measured as

vertical distance to the axis of the spinal cord (Fig. 1**B**). The parameter was measured in this manner because the graft constantly occupied a portion of the lesion gap. In each section, the values of 2 parts of scars separated by the graft were summed, and then normalized to be a percentage as divided by the width of spinal cord section. For the cavitation measurement, the rostra-caudal length of the biggest cavity was measured in each section. Values obtained from three sections per animal were averaged for statistical analysis. To evaluate grafted cell survival, the area of GFP-labeled graft within and adjacent to the lesion site was also quantified in the cords with grafts. The transplanted regions were imaged in 3 middle sections at 1.25 × 1.6 objectives, and then GFP^+area was outlined and measured using ImageJ software. The values in 3 sections were then averaged per rat for statistics. All data were presented as means ± SEM. Data were compared by ANOVA and LSD post hoc tests. A significance criterion of $p < 0.05$ was used.

3. Results

3.1. Tissue microaspiration causes a severe lesion gap and cavitation

When the spinal cord was dissected 8 weeks post-injury, we noticed that tissue grew and filled the lesion site of the spinal cord. In the spinal cord sections, immunostaining revealed most lesions were filled with PDGFR-β^+fibroblasts. The three groups of rats displayed markedly diverse lesion conditions. In the majority of cases that received cut + microaspiration (n = 6 in total of 7), the rostro-caudal extent of lesion is big and many PDGFR-β^+fibroblasts existed within the lesion (Fig. 2**A**). Immunostaining also demonstrated that the area was occupied by ECM (data not shown). The most prominent phenomenon in this group was the existence of large cavities nearby the host tissues. The number of cavities ranged from 1 to 5 per section, which emerged in either the rostral or caudal part of the cord without preference. One case even had large cavities in the host tissue adjacent to the lesion.

On the contrary, lesions that received cut without microaspi-ration were small, which were identified by interrupted GFAP labeling (Fig. 2**B**). Massive PDGFR-β^+fibroblasts invaded the lesion gap in all sections from dorsal to ventral. Most spinal samples (n = 7 in total of 11) in the group of cut alone did not show big cavities around the lesion site, except the occasional incidence of small holes. Two cases had spared spinal tissue identified by continuous $GFAP^+$ labeling crossing lesion in the ventral or lateral part, suggesting an incomplete injury, which were excluded from quantitative analysis. In most crushed cords (n = 4 in total of 5), dense PDGFR-β^+fibroblasts filled the lesion gap and some small cavities were present within the vicinity (Fig. 2**C**). Under high magnification, PDGFR-β^+fibroblasts were co-labeled with DAPI within the lesion site, verifying their cellular property. $GFAP^+$ astrocyte processes penetrated into fibrotic scars and stopped there (Fig. 2**D**, **E**). Statistical analysis demonstrated significantly greater rostro-caudal distances of fibrotic scars (cut + microaspiration 1045 ± 134.8 μm vs. cut 418.5 ± 59.8 μm, $p < 0.001$; vs. crush 480.5 ± 101.7 μm, $p < 0.01$; Fig. 2**F**) and cavities (cut + microaspiration 529.8 ± 64.2 μm vs. cut 290 ± 43 μm; vs. crush 234.3 ± 69.6 μm, both $p < 0.01$; Fig. 2**G**) in rats treated with cut + microaspiration compared to the other two groups (oneway ANOVA, both $p < 0.01$, followed

by LSD post hoc). There was no statistical difference in the sizes of scars ($p = 0.59$) and cavities ($p = 0.54$) between the groups with cut alone and crush.

3.2. Cellular grafts rarely bridge a microaspirated lesion gap

Triple immunostaining was processed in the grafted samples to evaluate GFP$^+$transplanted cells, PDGFR-β$^+$fibrotic scars, and GFAP$^-$ cavities. In the cords that received cut + microaspiration, large tissue cavities were constantly observed nearby the lesion (Fig. 3**A**). Although some GFP$^+$ grafted cells survived, they were mostly located at the edge of cavity. Severe PDGFR-β$^+$ fibrotic scarring often separated the graft. GFP-labeled axons extended in the host tissue towards one direction opposite the scar. Indeed, the GFP$^+$cellular bridge was rarely perceived to perforate fibrotic scars in most cases (n = 5 in total of 6), suggesting that the rostrocaudal connection was not established for signal transmission. In the other two groups, however, graft-derived tissue bridges were frequently seen in the sections from dorsal to ventral, and GFP$^+$ axons persistently elongated into both sides of host neural tissue. In most cords treated with cut only (n = 7 in total of 9), GFP$^+$ grafts often occupied some lesion regions and linked both ends of spinal cord stumps even though PDGFR-β$^+$ fibroblasts jammed into part of the gap (Fig. 3**B**). The interface of graft/host lacked distinct boundaries of intense GFAP$^+$ astrogliosis, and small holes sometimes occurred in the graft/lesion site. Only 2 rats in those receiving cut alone showed big cavities in very few sections in which GFP$^+$ grafts hardly formed a tissue bridge. In all cords treated with crush (n = 4), GFP$^+$ grafts enabled to grow in the lesion site and blended extensively with the rostral and caudal cords (Fig. 3**C**). Such integration rendered difficulties to differentiate the interface of graft/host. Notably, fibrotic scars in the crushed lesion exhibited a dispersed distribution pattern. Most PDGFR-β-labeled fibrosis was located on the edge of bilateral sides of sections. Very small cavities occasionally appeared around the lesion or grafted site. In addition, some PDGFR-β$^+$ fibroblasts were present in GFP$^+$ grafts with tube-like shaped morphology implying genesis of nascent blood vessels (Fig. 3**D–F**).

Quantification analysis showed that the grafted cords receiving cut + microaspiration had a greater extent of fibrotic scarring (cut + microaspiration 0.95 ± 0.05% of spinal cord width vs. cut 0.55 ± 0.10% of spinal cord width, $p < 0.01$; vs. crush 0.32 0.03% of spinal cord width, $p < 0.001$; Fig. 3**G**) and larger size of ± cavities (cut + microaspiration 940 ± 140.9 μm vs. cut 327.1 ± 75.4 μm, $p < 0.001$; vs. crush 315 ± 74.0 μm, $p < 0.01$; Fig. 3**H**) compared to those treated with cut or with crush. There was no statistical difference in the size of scars ($p = 0.10$) or cavities ($p = 0.94$) between groups with cut and with crush. Statistical analysis also revealed a more than 2-fold larger GFP$^+$ area in cords receiving crush injury (0.201 ± 0.034 mm^2) compared to the other two groups (cut + microaspiration 0.083 ± 0.016 mm^2, $p < 0.001$; cut0.076 ± 0.009 mm^2, $p < 0.001$; Fig. 3**I**), indicating better survival of grafts in this injury model (one-way ANOVA, all $p < 0.001$, followed by LSD post hoc).

4. Discussion

Multiple factors influence lesion severity and graft survival in the injured spinal cord, such as injury-induced inflammatory response, quality and quantity of donor cells as well as

transplantation techniques (Reier et al., 1986; Medalha et al., 2014; Surey et al., 2014). Successful cell grafting can establish new neuronal circuits to relay signals across the lesion from higher centers to the caudal spinal cord (Lu et al., 2012). Actually, neural tissue bridging is the anatomical basis of potential functional recovery (Tuszynski et al., 2014). Under standard conditions, we compared the effect of different surgical techniques on lesion morphology and cellular transplantation. The results indicate that microaspiration, a widely used technique to produce complete SCI, often causes severe fibrotic scarring and large cavities, which prevents graft survival and integration with host neural tissue. In contrast, complete lesions induced by cut only or crush produced significantly less cavitation and greater survival of transplanted cells.

In order to achieve a complete SCI model for cell transplantation, investigators often use combinatorial surgical techniques for disrupting entire spinal tissue. After the dura is opened, we initially use iridectomy scissors to cut the spinal cord. Depending on researchers' techniques and experience, there is usually more or less spared tissue in the lesion. The presence of spared tissue can become artifacts in ensuing histological analysis for axon regeneration or sprouting, and also cause a problem for behavioral tests (Tuszynski and Steward, 2012). We usually aspirate the lesion cavity to remove potentially spared neural tissue using multiple types of self-made aspirators with tips of different diameters. However, the power of microaspiration is hard to control for consistency between animals. With our own experience, we alternately use the small and big aspirators for spared tissue. This unavoidably causes unanticipated tissue damage at the spinal cord stumps. Subsequently, tissue necrosis induces a heavy inflammatory response and macrophage infiltration, which initiates secondary damage in the adjacent spinal cord and leads to severe tissue destruction (Fitch et al., 1999). This could be a rational explanation as to why larger cavities persistently occurred in these rats. The interpretation is supported by the fact that, in cords receiving cut only or crush injury, the incidence of large cavitation is dramatically reduced. Although another group reported that aspiration of a contused spinal cord did not impair axonal growth into delayed peripheral nerve grafts (Sandrow et al., 2008), it does not mean this surgical technique is not harmful to cellular transplants in a completely-transected spinal cord.

Previous studies did not characterize the properties of nonneuronal partition separating the graft in the spinal cord (Sharp et al., 2014). It is now clear that the structure is mainly composed of numerous fibroblasts. As a healing process in response to traumatic spinal damage, vessel-derived fibroblasts invade the lesion, proliferate, and secrete a large amount of ECM to seal tissue deficits (Fernandez-Klett and Priller, 2014). Fibroblast migration is beneficial to nascent vessel genesis in the graft. On the other hand, the aggregation of these mesenchymal cells and their derivatives form fibrotic scars in the lesion, which is a physical barrier impeding axonal growth. For decades, it was thought that invading fibroblasts migrate from neighboring pia (meningeal)/arachnoid members. Nevertheless, recent studies disclosed that these cells mainly originate from perivascular cells in the adjacent parenchyma and they are specifically immunoreactive to an antibody against PDGFR-β (Goritz et al., 2011; Soderblom et al., 2013). If a severe injury causes extensive tissue damage, these invading fibroblasts are unable to proliferate sufficiently to fill the tissue deficit. This was observed in most cases treated with cut + microaspiration, in which fibrob-

lasts sparsely distribute into ECM-like structures in the most parts of the lesion. When fetal cells are grafted into this large tissue gap, it is difficult for them to survive probably because fibroblast-based angiogenesis rarely occurs here. By contrast, most cases that received cut only or crush injury had narrower scars and much smaller cavities. Grafted cells frequently created a tissue bridge across the lesion connecting the rostral and caudal cord ends, indicating the possibility of signal transmission. The variability in cell engraftment corresponds to various situations of injury. That is to say, the extent of local tissue damage largely influences grafted cell survival, growth, and fusion to the host spinal cord. In addition, it is not ideal to remove formed fibrotic scars for cell grafting in the chronic stage since the treatment may result in excessive tissue damage and the emergence of large cavities. This was reported in the replication study (Sharp et al., 2014) whereas Lu and colleagues' original research did not perform the experiment (Lu et al., 2012).

In the present study, aspiration was done in the groups receiving cut + microaspiration with or without cell graft. This technique was only used to remove lateral and ventral spared spinal cord tissues after cutting with scissors, but not at the rostral and caudal lesion edges. Following aspiration, the rostrocaudal extent of the lesion immediately after the injury was similar in these animals compared to animals from the cut only group, indicating that the increased lesion size in aspirated spinal cords resulted from secondary degeneration and not from the surgery itself.

5. Conclusions

In summary, varying outcomes in cell transplantation for SCI may result from surgical techniques used for lesioning. Particularly, microaspiration can cause tissue damage and induce severe fibrotic scars and cavitation, however the growth inhibitory factors are less severe when cut alone or crush techniques are used. In the future, it may be vital to explore more effective strategies to avoid scarring and cavitation for a higher success of cell transplantation.

Acknowledgments

We gratefully thank Dr. Hisham Sharif for proofreading the manuscript. Support for this work was provided by the US National Institution of Health (NIH NINDS, R01NS099076), Craig H. Neilsen Foundation (280072), and Morton Cure Paralysis Funds (MCPF) to S.H. and the US NIH NINDS (R01NS085426) and DoD/CDMRP W81XWH-14-1-0605 to V.J.T.

References

Blesch A, Tuszynski MH, 2003 Cellular GDNF delivery promotes growth of motor and dorsal column sensory axons after partial and complete spinal cord transections and induces remyelination. J. Comp. Neurol 467, 403–417. [PubMed: 14608602]

Fernandez-Klett F, Priller J, 2014 The fibrotic scar in neurological disorders.Brain Pathol 24, 404–413. [PubMed: 24946078]

Fitch MT, Doller C, Combs CK, Landreth GE, Silver J, 1999 Cellular and molecular mechanisms of glial scarring and progressive cavitation: in vivo and in vitro analysis of inflammation-induced secondary injury after CNS trauma. J. Neurosci 19, 8182–8198. [PubMed: 10493720]

Gaillard A, Prestoz L, Dumartin B, Cantereau A, Morel F, Roger M, Jaber M,2007 Reestablishment of damaged adult motor pathways by grafted embryonic cortical neurons. Nat. Neurosci 10, 1294–1299. [PubMed: 17828256]

Goritz C, Dias DO, Tomilin N, Barbacid M, Shupliakov O, Frisen J, 2011 A pericyte origin of spinal cord scar tissue. Science 333, 238–242. [PubMed: 21737741]

Hou S, Tom VJ, Graham L, Lu P, Blesch A, 2013 Partial restoration of cardiovascular function by embryonic neural stem cell grafts after complete spinal cord transection. J. Neurosci 33, 17138–17149. [PubMed: 24155317]

Jakeman LB, Reier PJ, 1991 Axonal projections between fetal spinal cord transplants and the adult rat spinal cord: a neuroanatomical tracing study of local interactions. J. Comp. Neurol 307, 311–334. [PubMed: 1713233]

Lepore AC, Fischer I, 2005 Lineage-restricted neural precursors survive, migrate, and differentiate following transplantation into the injured adult spinal cord. Exp. Neurol 194, 230–242. [PubMed: 15899260]

Lu P, Wang Y, Graham L, McHale K, Gao M, Wu D, Brock J, Blesch A,Rosenzweig ES, Havton LA, Zheng B, Conner JM, Marsala M, Tuszynski MH, 2012 Long-distance growth and connectivity of neural stem cells after severe spinal cord injury. Cell 150, 1264–1273. [PubMed: 22980985]

Medalha CC, Jin Y, Yamagami T, Haas C, Fischer I, 2014 Transplanting neural progenitors into a complete transection model of spinal cord injury. J. Neurosci. Res 92, 607–618. [PubMed: 24452691]

Reier PJ, Bregman BS, Wujek JR, 1986 Intraspinal transplantation of embryonic spinal cord tissue in neonatal and adult rats. J. Comp. Neurol 247, 275–296. [PubMed: 3522658]

Reier PJ, 2004 Cellular transplantation strategies for spinal cord injury and translational neurobiology. NeuroRx 1, 424–451. [PubMed: 15717046]

Sandrow HR, Shumsky JS, Amin A, Houle JD, 2008 Aspiration of a cervical spinal contusion injury in preparation for delayed peripheral nerve grafting does not impair forelimb behavior or axon regeneration. Exp. Neurol 210, 489–500. [PubMed: 18295206]

Sharp KG, Yee KM, Steward O, 2014 A re-assessment of long distance growth and connectivity of neural stem cells after severe spinal cord injury. Exp. Neurol 257, 186–204. [PubMed: 24747827]

Soderblom C, Luo X, Blumenthal E, Bray E, Lyapichev K, Ramos J, Krishnan V, Lai-Hsu C, Park KK, Tsoulfas P, Lee JK, 2013 Perivascular fibroblasts form the fibrotic scar after contusive spinal cord injury. J. Neurosci 33, 13882–13887. [PubMed: 23966707]

Surey S, Berry M, Logan A, Bicknell R, Ahmed Z, 2014 Differential cavitation, angiogenesis and wound-healing responses in injured mouse and rat spinal cords. Neuroscience 275, 62–80. [PubMed: 24929066]

Tuszynski MH, Steward O, 2012 Concepts and methods for the study of axonal regeneration in the CNS. Neuron 74, 777–791. [PubMed: 22681683]

Tuszynski MH, Wang Y, Graham L, McHale K, Gao M, Wu D, Brock J, Blesch A, Rosenzweig ES, Havton LA, Zheng B, Conner JM, Marsala M, Lu P, 2014 Neural stem cells in models of spinal cord injury. Exp. Neurol 261, 494–500. [PubMed: 25079369]

HIGHLIGHT

- Surgical technique of microaspiration in SCI results in severe scarring and huge cavities.
- Neural tissue bridging rarely occurs after grafting embryonic brainstem cells into the microaspirated lesion.
- Crush injury prevents severe cavitation, and facilities grafted cell survival and integration.

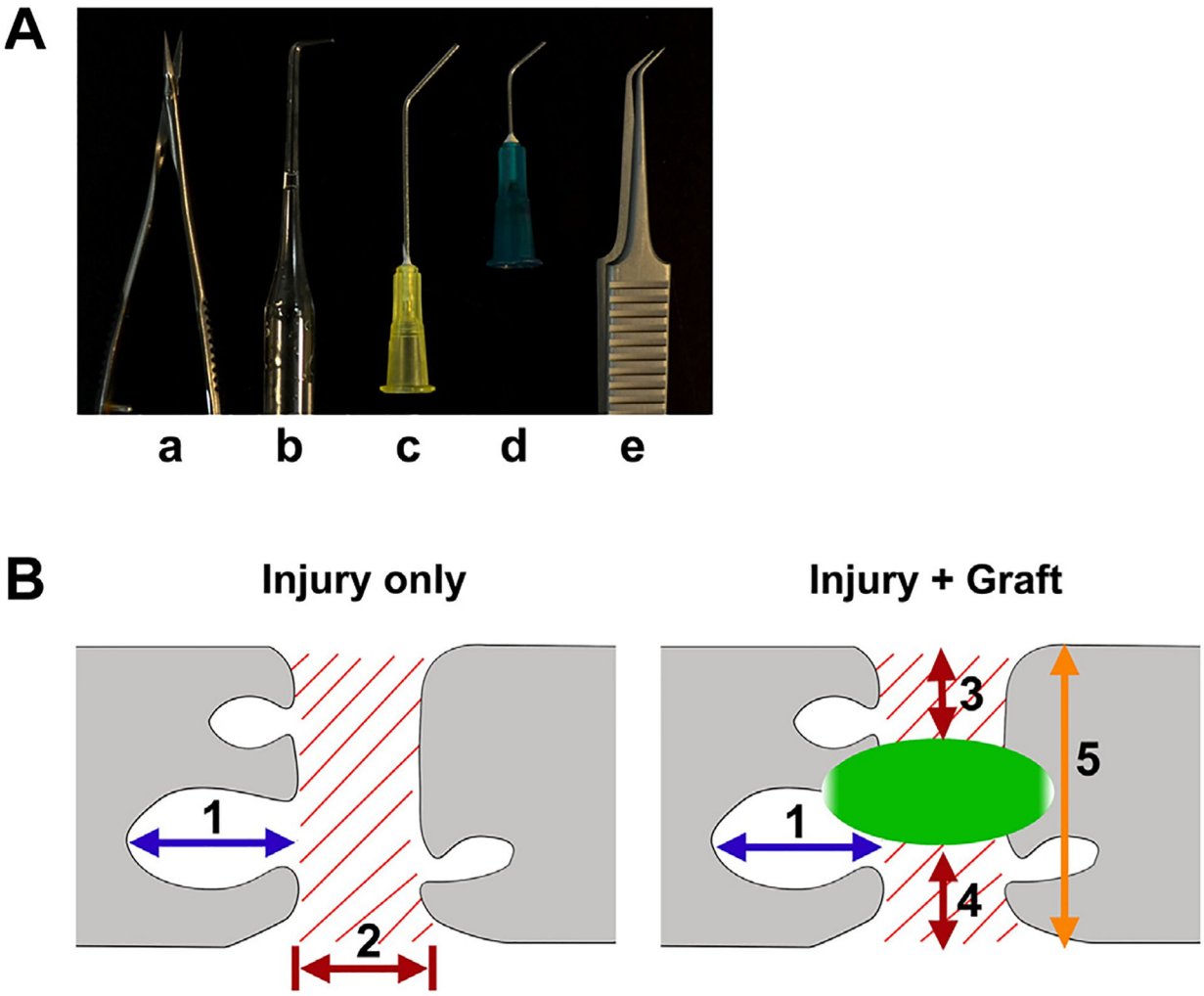

Fig. 1.

Surgical tools (**A**) to create a complete SCI include (**a**) iridectomy microscissors, (**b–d**) three self-made aspirators with different diameters in the tip, and (**e**) fine forceps for crush. Schematic diagrams (**B**) illustrate how the sizes of cavities (**1**) and fibrotic scars (**2** or **3**) were measured. The size of cavity is referred to the rostrocaudal distance (**1**) of the biggest one in each section. The rostro-caudal distance of fibrotic scarring (**2**) in lesion is defined in the spinal cord with injury only, while the vertical depth of fibrotic scars (**3 + 4**) is scaled and divided by the width of the section (**5**) in grafted cords.

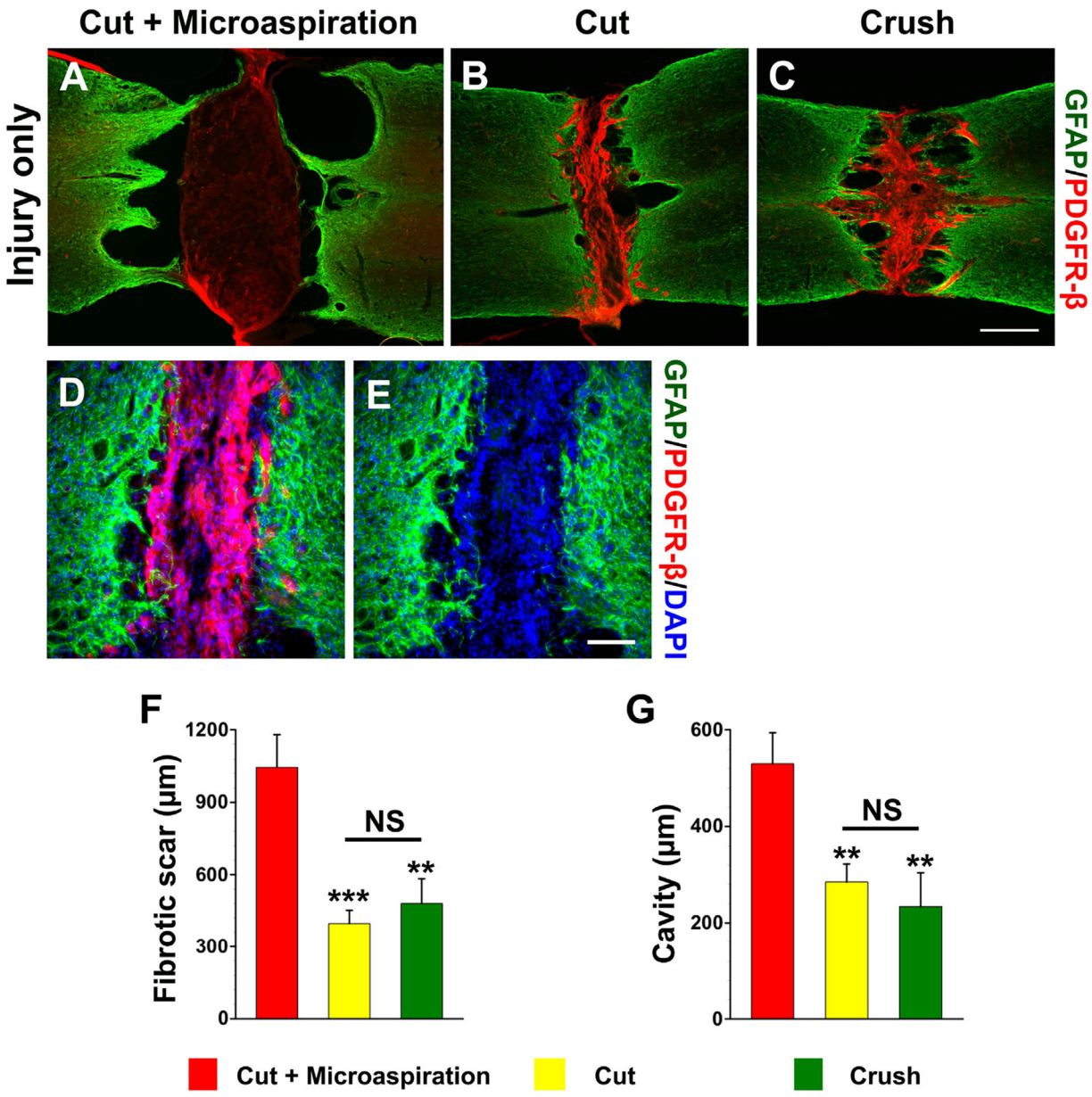

Fig. 2.

Lesion situations are variable with different surgical techniques in the cohort of injury only. A large lesion gap and cavities often occur in cords treated with cut + microaspiration; PDGFR-β^+ fibroblasts sparsely scatter in the lesion gap (**A**). However, most cords receiving (**B**) cut only or (**C**) crush exhibit a narrow lesion filled with dense fibroblasts; big cavities are rarely detected except a few small holes in the interface of scar/cord stump. (**D**, **E**) At high magnification, numerous PDGFR-β^+ fibroblasts occupy the lesion in a cord transected with cut without microaspiration. Statistical analysis shows that significantly (asterisks) larger sizes of (**F**) fibrotic scars or cavities (**G**) in rats receiving cut + microaspiration than other two groups (one-way ANOVA followed by LSD post hoc, $^{**}p < 0.01$, $^{***}p < 0.001$, NS $p > 0.05$). Scale bars: **C**, 0.5 mm; **E**, 100 μm.

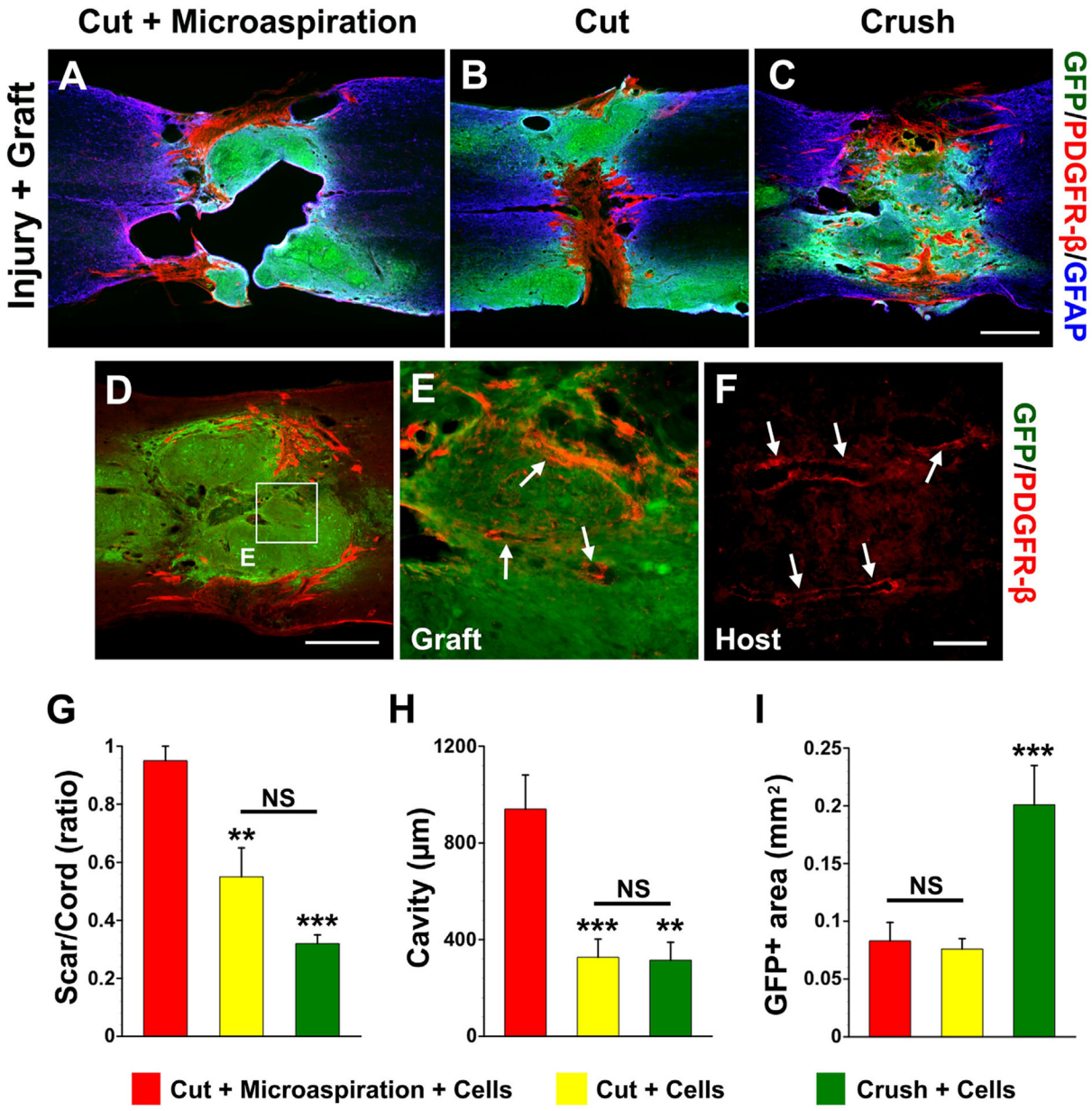

Fig. 3.

Scarring, cavitation and cell survival after embryonic BS-NSC transplanting. Eight weeks after cellular transplantation into the lesion site, a PDGFR-β-labeled fibrotic scar rift and large cavities separate GFP$^+$ grafts in cords receiving (**A**) cut + microaspiration. In contrast, the graft in cords treated with (**B**) cut only or (**C**) crush forms a neural tissue bridge across the non-neural scar. Interestingly, some PDGFR-β-labeled fibroblasts are associated with (**D**, **E**) vessel-like structures (arrows) within GFP$^+$ grafts, which are similar to (**F**) labeled real blood vessels (arrows) in the host tissue of same section. **E** is higher magnification of boxed region in **D**. Statistical analysis shows that the sizes of (**G**) fibrotic scars or cavities (***H***) are significantly larger in rats receiving cut + microaspiration than other two groups. Furthermore, quantification of the size of graft demonstrates that a larger GFP$^+$ area in cords

receiving crush injury compared to other two groups (**I**), indicating better survival of grafts in this injury model. (one-way ANOVA followed by LSD post hoc, $^{**}p < 0.01$, $^{***}p < 0.001$, NS $p > 0.05$). Scale bars: **C**, 0.5 mm; **D**, 100 μm; **F**, 70 μm.